Transaction B: Mechanical Engineering
Vol. 17, No. 5, pp. 395–405

Research Note

SCIENTIA IRANICA

Aerodynamic Investigation of a Damaged Airfoil with Wall Effects

F. Rasi Marzabadi[1], B. Beheshti Boroumand[1,*], M. Mani[1] and F. Ajalli[1]

Abstract. *Aerodynamic behavior of an airfoil with circle, right and inverse triangle shaped damage was numerically investigated. The flow through the damage was driven by the pressure differential between the upper and lower wing surfaces. For all damage shapes, the results showed that the flow could be categorized as weak or strong jets. The jet exited the rear of the damage; its size was determined by the width of the rear part of the hole and was dependent on the shape of the damage. Generally, when compared with an undamaged model, increasing the angle of attack for a damaged model resulted in increased loss of lift coefficient, increased drag coefficient and more negative pitching moment coefficient. This effect was more severe for the right triangle case. Furthermore, the numerical results were compared with experimental data to study the effect of a wall on the flow field.*

Keywords: *Aerodynamics; Damage; Airfoil; Weak jet; Strong jet; Wall effect.*

INTRODUCTION

One of the key design requirements is aircraft survivability. Survivability of the aircraft is dependent upon its vulnerability to damage caused by a variety of threat types, ranging from small arms, through to anti-aircraft artillery and missiles. During the aircraft design stage, survivability enhancement techniques are implemented, which include assessment of the capabilities of aircraft to survive levels of battle damage caused by impacts from conventional weapons. As a part of this process, vulnerability assessment has tended to concentrate mainly on structural integrity, while only paying secondary attention to the actual aerodynamic effects of damage to wings or control surfaces. This lack of attention to aerodynamic factors may, in part, be attributed to the unavailability of relevant data [1].

The shape of the damage depends on the mechanism by which the damage is produced and the material from which the body is manufactured. For many forms of damage, the resulting shape consists of a circular center with radial radiating of the cracks. If the body is metallic, the damage is accompanied by petaline, where the metal is bent over. For composite material, the damage is accompanied by delamination, which lies in the plane of the punctured material [1].

When the wing is damaged, it effectively generates a flow path through the wing structure between regions of high and low pressure. So, it influences the aerodynamic characteristics [2].

Only a limited number of studies on the aerodynamics of battle damage wings have been published in the literature. Hayes [2] studied the effect of damage on swept-wing airplanes in 1968. In 1995, Irwin et al. [3] tested damaged solid airfoils through a wind tunnel. Irwin and Render in 1996 [4] studied the aerodynamic effects and flow structure of different circular damage shapes. These circular shapes had different percentages of chord as diameter and four different positions on the chord. He identified that the flow through the damage was of two types and dependent on the angle of attack and the size of the damage. The types were named "weak jet" and "strong jet", which was terminology adapted from investigations into "jet-in-cross flow". Robinson and Leishman [5] in 1997 studied the effect of ballistic damage on the aerodynamics of a helicopter rotor airfoil. He found that damage degraded the aerodynamic performance of the airfoils with a mild decrease in lift but major increases in drag. In 2005,

1. *Aerospace Research Institute, Tehran, P.O. Box 14665-834, Iran.*
*. *Corresponding author. E-mail: beheshti@aut.ac.ir*

Received 12 September 2009; received in revised form 1 March 2010; accepted 6 July 2010

Render and Walton [6] investigated the aerodynamic effects of flap, chamber, and repair schemes on damaged wings. In the same year, Mani and Render [7] implemented some experiments to determine the effect of triangle and star shaped damage on the aerodynamic characteristics of infinite wings. These experiments took place in the low turbulent wind tunnel at the Aeronautical and Automotive Engineering Department of Loughborough University. It is an open circuit wind tunnel test section, with dimensions of 450×450 mm^2, maximum velocity of 40m/s and a turbulent level of typically 0.1%. A three component balance was located beneath the working section, with an accuracy of 0.1% of measured force and pitching moment for each component. The experiments were conducted at a velocity of 35 m/s, corresponding to the Reynolds number of about 500,000 [7].

They showed that for all damage shapes, the jet exited the rear of the damage and its size was determined by the width of the rear part of the hole; the main features of the flow were identified as those previously described by Irwin for circular damage.

In this study, the flow is numerically investigated on a section of NACA 64_1-412 airfoil with circle, right and inverse triangle shapes of damage, and also the effect of test section walls on the experimental results obtained from [7] is studied.

NUMERICAL FLOW SIMULATION

Numerical modeling and analysis of the flow around the damaged wing section is investigated using a commercial CFD code.

Geometry

The model of study is a section of NACA64_1-412 airfoil with 200 mm chord and 450 mm span. The shapes of the damages are circle, right and inverse triangle, through the airfoil and normal to the chord. The center of the damage is put on a point at the mid-span and mid-chord of the model. The circle has 20% chord diameter (40 mm) and the areas of the triangles are equal to the circle areas, so there is a length of 54 mm for each side. Three geometries of the damaged wing sections are shown in Figure 1. Note that when the apex of the triangle is nearer to the leading edge of the airfoil, the damage shape is called "right triangle" (Figure 1a), and when the apex of the triangle is nearer to the trailing edge of the airfoil, the damage shape is called "inverse triangle" (Figure 1c).

Grid

For two shapes of damage, an unstructured grid of tetrahedral cells is used for the entire solution domain

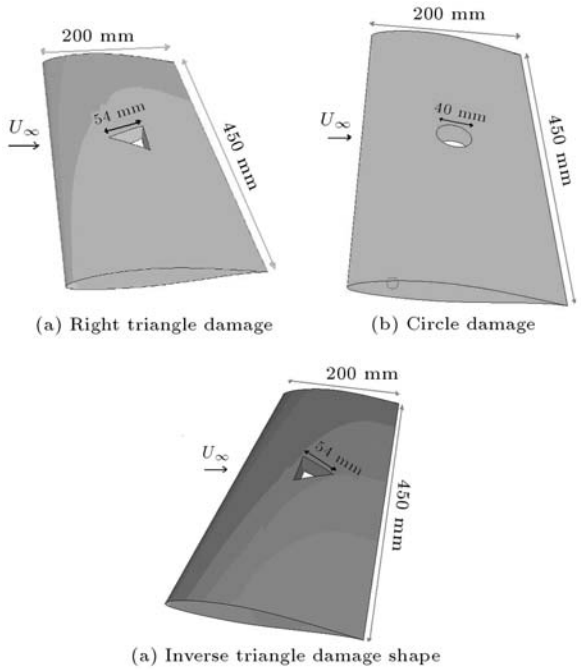

(a) Right triangle damage (b) Circle damage

(a) Inverse triangle damage shape

Figure 1. Geometry of the damaged airfoil model.

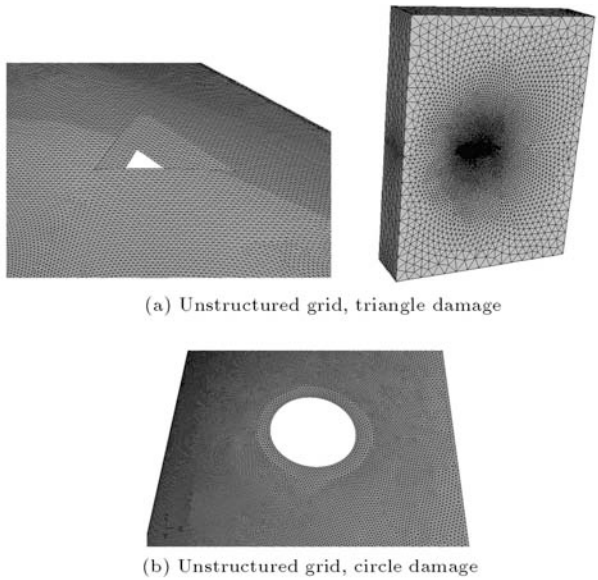

(a) Unstructured grid, triangle damage

(b) Unstructured grid, circle damage

Figure 2. Grids with resolution of the smallest cells adjacent to the airfoil surface.

(Figure 2). A trade-off between computation time and quality of results on and near the surface of the model led to a grid with the smallest cells adjacent to solid walls, and the largest cells adjacent to inlet and outlet boundaries. The total number of cells in the unstructured grid is 1,787,078. Two finer grids with 2,916,972 cells and 4,545,916 cells have also been generated to study the effect of grid size on the results.

Figure 3 shows a grid study on two sensitive parameters of turbulence intensity and turbulence kinetic

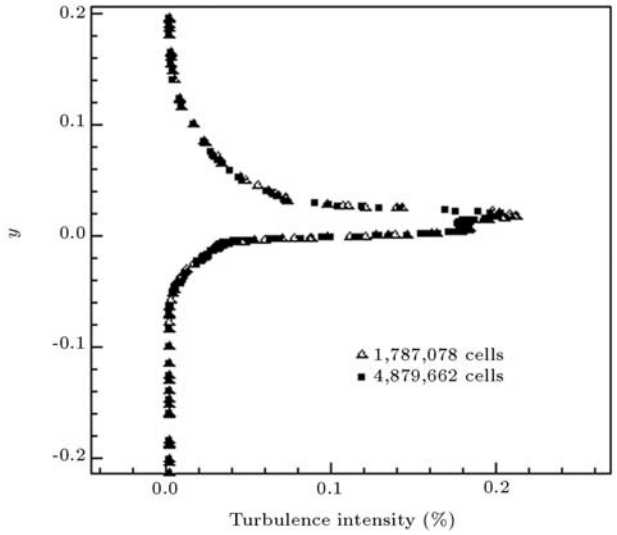

(a) Turbulence intensity distribution

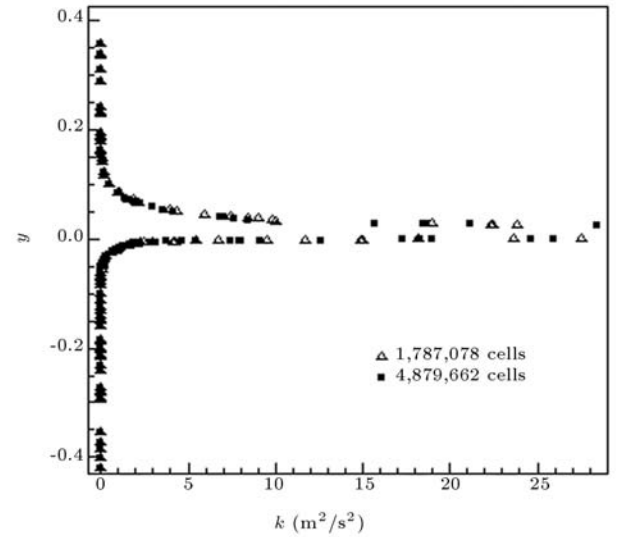

(b) Turbulence kinetic energy distribution

Figure 3. Grid study on two sensitive parameters, right triangle damage shape, $\alpha = 6°$.

energy. These parameters are studied in the middle of the model in the direction perpendicular to the chord. It is seen that increasing the size of the grid from 1,787,078 to 4,879,662 cells does not affect the distribution of these parameters, which means that the numerical results are independent of the grid size, and applying a grid size of 1,787,078 cells has sufficient accuracy.

Boundary Conditions

Three types of boundary condition are used: velocity inlet, outflow and wall. In order to distinguish domain boundaries, blue planes are used for the velocity inlet and the red plane for outflow (Figure 4). The magnitude of the velocity at the inlet is 35 m/sec, the operating pressure is 101325 Pa and the turbulent intensity is 0.1%, which relates to the experimental test condition of the model [7] that, here, is numerically investigated.

Note that for investigating wall effects the upper and lower walls of the test section (450×450 mm^2) are modeled separately for all angles of attack examined here. For other models, the size of the domain at each side is set to six times the chord length of the airfoil, which is big enough to damp turbulences before reaching the domain boundaries.

Numerical Solution Characteristics

The flow in this analysis is assumed to be steady, incompressible and turbulent. Employed equations include continuity and momentum conservation equations. Since there is no heat transfer in fluid, the energy equation is not applicable. For modeling of viscous turbulent flow, the $k - \varepsilon$ turbulence model is applied, since it has shown an excellent performance in many industrial relevant flows and is well established. Two transport equations (partial differential equations) are solved in this model: one for turbulent kinetic energy (k) and the other for the damping rate of turbulent kinetic energy (ε). The SIMPLE algorithm is applied to solve these two equations. Standard wall functions are also used for the areas close to the wall. It is noticeable that the wall functions are sensitive to the distance from the wall or y^+ parameter. Using an excessively fine mesh near the walls should be avoided, because the wall functions cease to be valid in the viscous sub-layer. The y^+ is chosen so that there would be at least a few cells inside the boundary layer; it is close to 30 in our model. The turbulence length scale in the turbulent model is defined equal to the chord

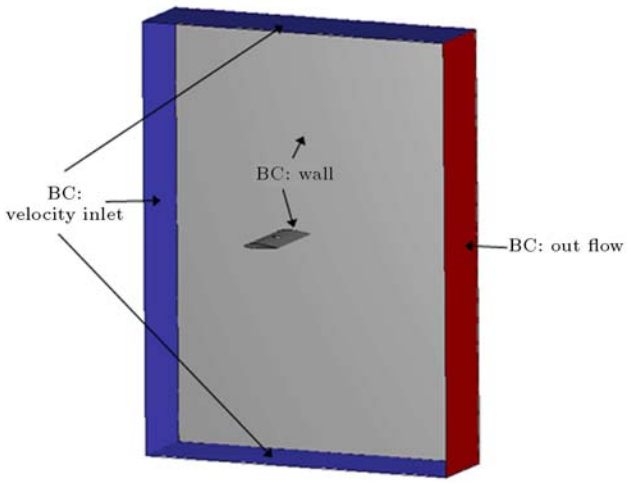

Figure 4. Boundary conditions.

length (0.2 m), and the operating pressure is assumed to be 101325 Pa.

RESULTS AND DISCUSSION

Qualitative and quantitative results of the numerical flow simulation are presented. It is carried out for all shapes of the damages (circle, right and inverse triangle) and the wall effects. Ten angles of attack from -2° to 16° (in 2° steps) were analyzed.

Qualitative Study of the Results

The flow through the damage is formed in two types, and is dependent on the angle of attack. These types are called by the names, 'weak jet' and 'strong jet'. Figure 5 shows an illustration of the characteristics of these two types. At the point where the surface flow meets the jet, an adverse pressure gradient is created, causing separation ahead of the damage hole, i.e. the forward separation line. Between this and the front of the damage hole, lays a vortex located between the forward and secondary separation lines. This is seen to wrap around to form a 'horse-shoe' vortex (terminology used by jets-in-cross flow investigations [8,9]). A region of upstream 'reversed flow' is also present where the flow through the damage pushes forward from the damage hole. Flow in this region is subsequently entrained rearwards, and added to the damage wake. At the rear edge of the damage hole, there are two vortex centers observed to be contra-rotating. The exact position of the vortex centers varies with jet strength moving forward around the damage edge

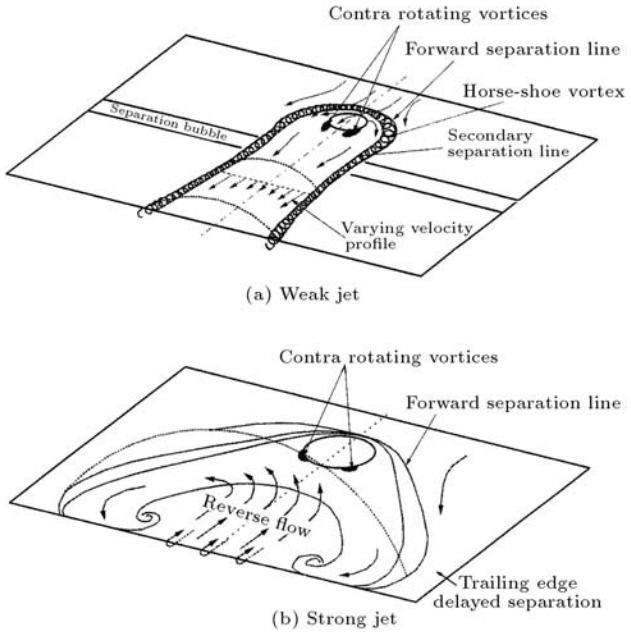

Figure 5. Weak and strong jet characteristics.

with increasing the angle of attack, but remaining approximately symmetrical about the centerline of the hole. Downstream of the hole, the damage wake attaches to the surface, cutting through the laminar separation bubble. The flow in the wake is moving in a free stream direction, however, there appears to be a surface velocity gradient within the wake from the centerline outwards. This results in the edges of the wake having a greater velocity than the center. The main characteristic of the 'weak jet' is that the flow exits at the rear edge of the hole, and is immediately bent over, forming a wake that is attached to the upper surface. As the angle of attack is increased, the jet no longer immediately bends over upon exiting the hole. Instead, it penetrates into the flow above the upper surface. This increases penetration into the free stream flow and results in the jet detaching from the surface, causing a separated region. This region exists between the jet and upper wing surface, extending from immediately behind the damage to the trailing edge. Within this region, the flow is highly three dimensional with a large extent of reverse flow. This flow type is named 'strong jet' whose characteristics are illustrated in Figure 4b. The main surface flow features are as follows. Both forward and secondary separation lines are again seen upstream of the damage. Although the surface flow immediately upstream of the damage is turbulent, the separation lines show little change in position relative to the damage, from those of the weak-jets. Moving chord wise, the track of the separation lines and the associated vortex deflect into a horse-shoe configuration, with a span wise extent greater than that seen in the weak-jets. This significant increase in wake size indicates the extent of the large region of reverse flow beneath the detached strong-jet. Again, two contra-rotating vortices are located at the damage edge. These have moved forward around the edge of the damage from the previous weak-jet locations. The dividing line between wake and undisturbed wing surface flow ends with two large contra-rotating vortices located close to the trailing edge. It appears that the wake entrains fluid from the surrounding upper surface flow, and around the trailing edge from the lower wing surface. The entrainment of undisturbed upper surface flow into the wake appears to delay the onset of trailing edge separation either side of the wake. Such trailing edge separation has previously been seen on the undamaged wing.

In Figures 6 to 10, the velocity vectors are shown for various damage shapes at two angles of attack of 0 and 10 degrees in both side and top views.

Figures 6 and 7 show the velocity vectors around the right triangle and circle damaged airfoils, respectively, from the side view for both weak and strong jet cases. It is seen that at $\alpha = 0°$, there is a weak jet exiting the damage hole, which formed an

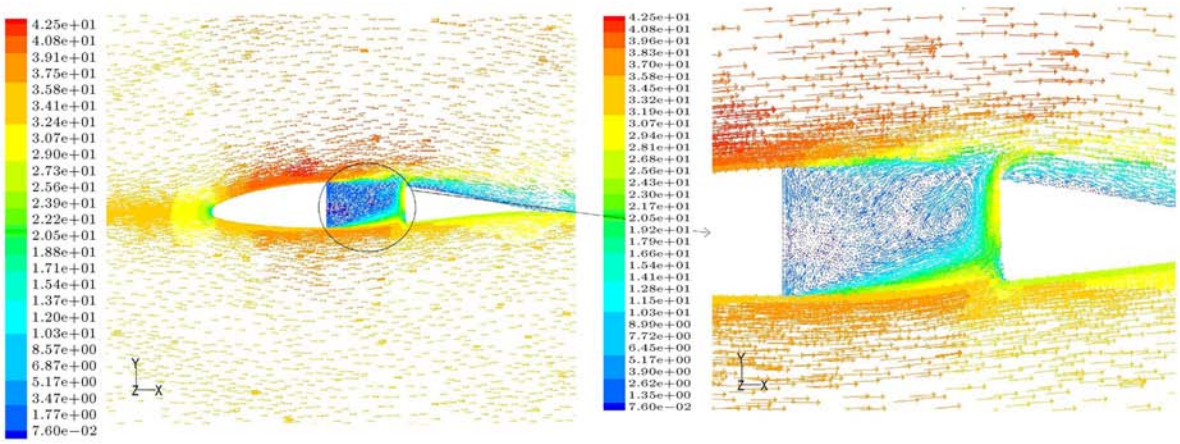

(a) Weak jet, $\alpha = 0°$

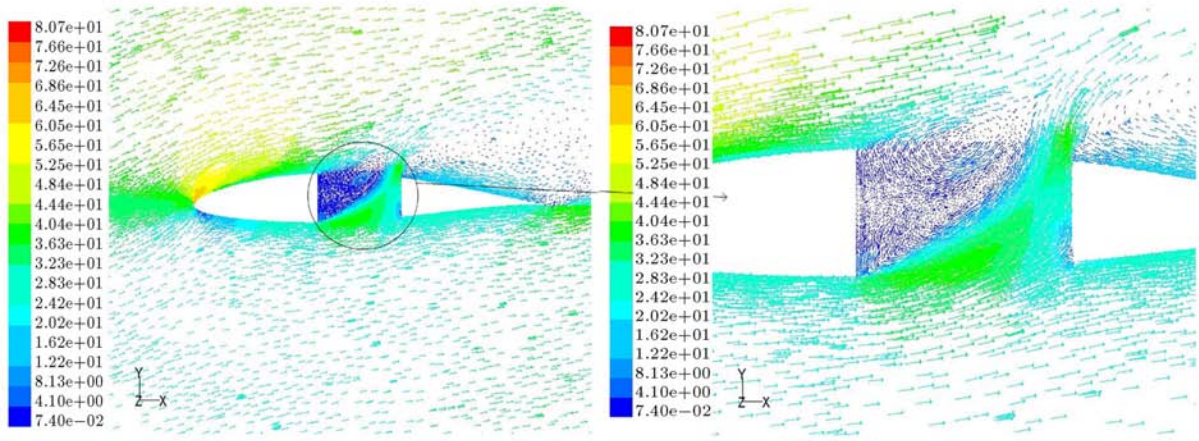

(b) Strong jet, $\alpha = 10°$

Figure 6. Velocity vectors, side view, right triangle damage.

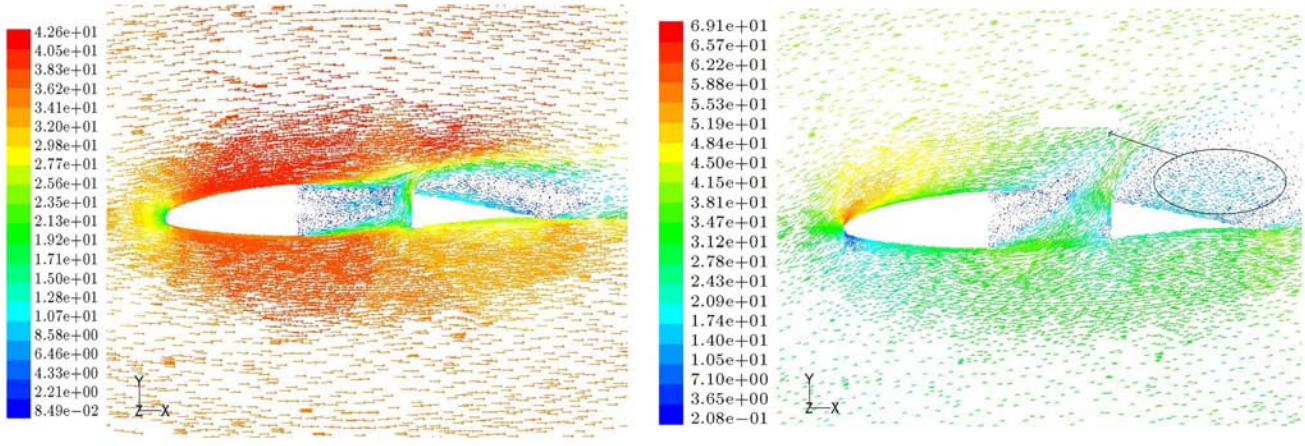

(a) $\alpha = 0°$ (b) $\alpha = 10°$

Figure 7. Velocity vector, side view, circle damage.

attached wake behind the damage hole. Because of the pressure difference between two surfaces of the airfoil, the flow would like to penetrate from the lower surface of the airfoil to the upper surface and this flow through the damage pushed forwards from the damage hole and added to the damage wake. At $\alpha = 10°$, the jet no longer immediately bent over upon exiting the hole and penetrated to the free stream. Finally, a separated region is formed between the jet and upper wing surface. Figures 6b and 7b show

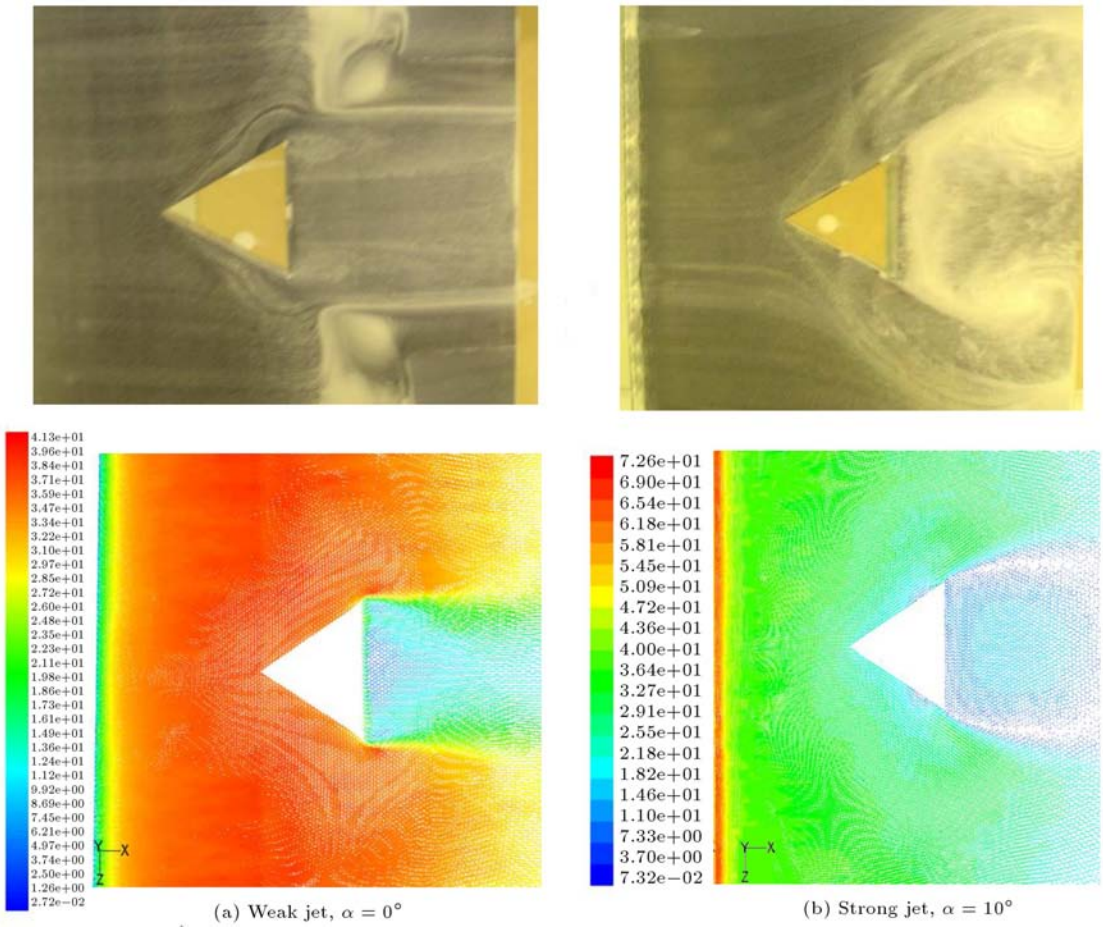

(a) Weak jet, $\alpha = 0°$ (b) Strong jet, $\alpha = 10°$

Figure 8. Velocity vectors, top view, right triangle damage (the top figures are experimental results from [7]).

the separated region and detached wake of the strong jet.

In Figures 8 to 10, it is seen from top views of the velocity vector at the rear edge of the damage hole, as mentioned before, there are two vortex centers observed to be contra-rotating, which are the result of interaction between jet flow exiting the damage and free stream. The exact position of the vortex centers varied with jet strength, moving forward around the damage edge when increasing the angle of attack, but remaining approximately symmetrical about the damage centerline. At $\alpha = 0°$, downstream of the hole, the wake is attached to the surface. At $\alpha = 10°$, the wake size increase indicated the extent of the large region of reverse flow beneath the detached strong jet. The results of the experiments from flow visualization [7] are also indicated for qualitative comparison. As seen, there is a good agreement between the numerical and experimental results, qualitatively. Furthermore, it is seen that the size of the wake region downstream of the damage is changed due to the damage shape. For a fixed angle of attack, the jet size is dependent on the shape of the damage and is determined by the width of the rear part of the hole.

In order to grasp the flow field inside the damage hole, path lines of the circle damage shape at the middle section, at two angles of attack of 0 and 10 degrees, are illustrated in Figure 11. It demonstrates that the jet flow exit from rear portion of the damage hole. There is a low pressure region in the front portion of the hole and because of the suction of flow in this region, two groups of rotating vortices are formed inside the hole. The lower group of vortices rotates in a clockwise direction and the upper vortices rotate in a counterclockwise direction. Because the flow is pierced into the hole from both upper and lower surfaces of the airfoil, two groups of vortices are in opposite directions. The strike between the fluid and the front wall of the damage hole has the same structure as the collision of a flat plate and fluid flow. As the incidence angle increases to 10 degrees, there would be a stronger jet, and thus the position of these two groups of vortices changes, as they intend to become nearer to the front wall of the hole and also the angle of these counter rotating vortices increases relative to the horizon (Figure 11b).

Figure 12 shows a comparison between the chord wise pressure distribution of the damaged (right trian-

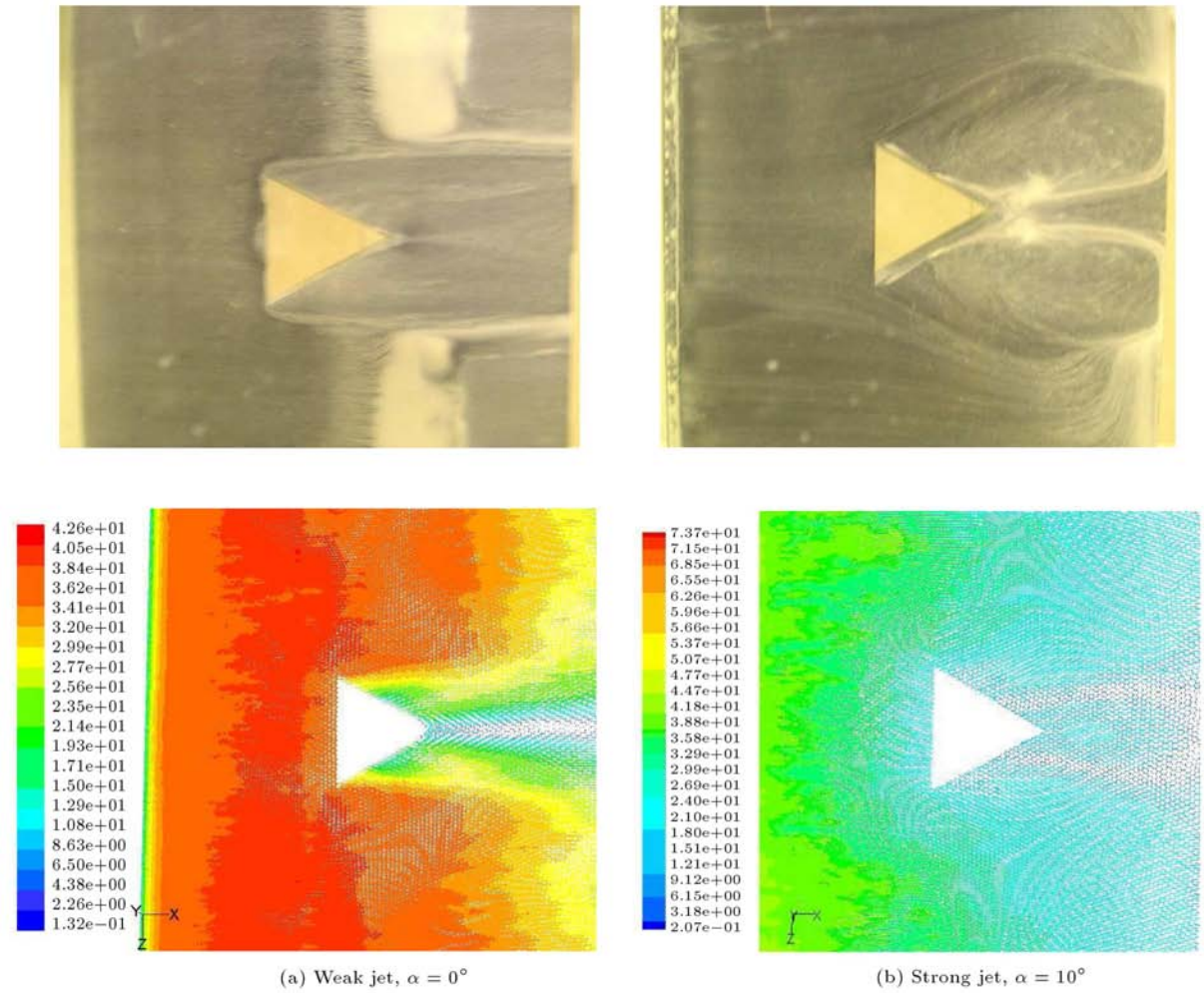

(a) Weak jet, $\alpha = 0°$ (b) Strong jet, $\alpha = 10°$

Figure 9. Velocity vectors, top view, inverse triangle damage (the top figures are experimental results from [7]).

gle) and undamaged airfoil at mid-span for two angles of attack: 0 and 10 degrees. There is an increased influence of damage with increasing angle of attack, i.e. the pressure differential across the damage increases. At zero angle of attack, when there is less flow through the damage, the pressure distribution shows only small changes with respect to the undamaged case in the immediate vicinity of the hole. As the pressure differential across the damage increases and the flow through the damage increases, it is consistent with both reductions in upper surface pressure peak suction, and development of the damage wake region.

Force and Moment Coefficients

Figure 13 shows the lift coefficient of damaged and undamaged models. It is seen that increasing jet strength with angle of attack generally results in an increased loss of lift coefficient. Furthermore, for damaged airfoil, due to turbulent; effects, the stall promotes to higher angles of attack from about 12° in the undamaged model to about 14° in the damaged one. In general, adding damage decreases $Cl_{\max}$ and slightly increases the stall angle of attack. The presence of damage also produces more drag and more negative (nose down) pitching moment.

Figure 14 shows aerodynamic coefficient increments due to three different damage shapes versus angle of attack. These coefficients are described as follows:

$$dCl = Cl_{\text{damaged}} - Cl_{\text{undamaged}},$$

$$dCd = Cd_{\text{damaged}} - Cd_{\text{undamaged}},$$

$$dCm = Cm_{\text{damaged}} - Cm_{\text{undamaged}}.$$

It is seen that due to the damage, the lift and pitching moment coefficients decrease, resulting in negative dCl and dCm. But, the drag coefficient increases and positive dCd is obtained. Furthermore, as mentioned before, increasing jet strength with angle of attack generally results in increased loss of lift coefficient, increased drag coefficient and more negative pitching moment coefficient increments. This is obvious from

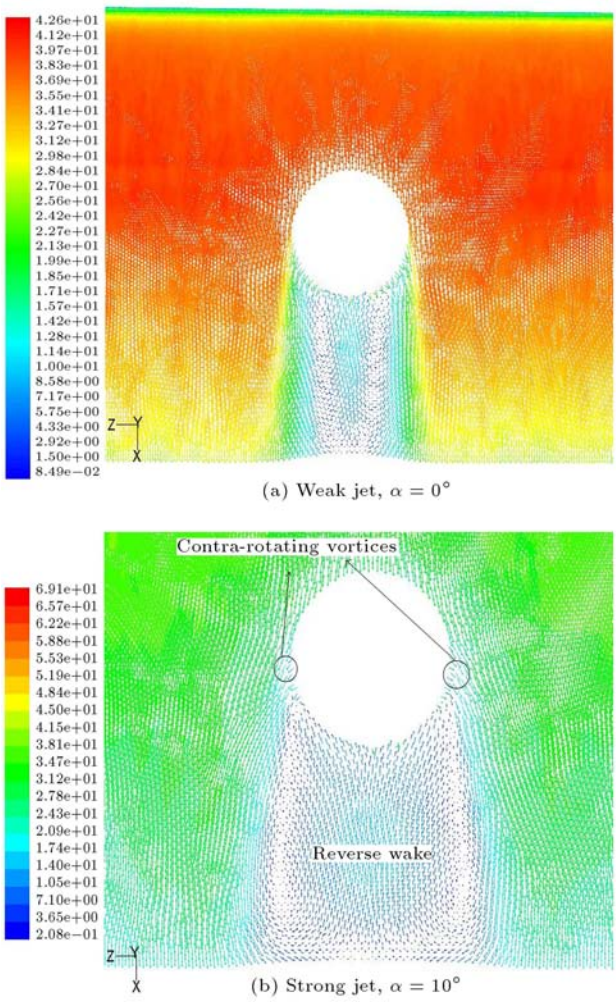

Figure 10. Velocity vector, top view, circle damage.

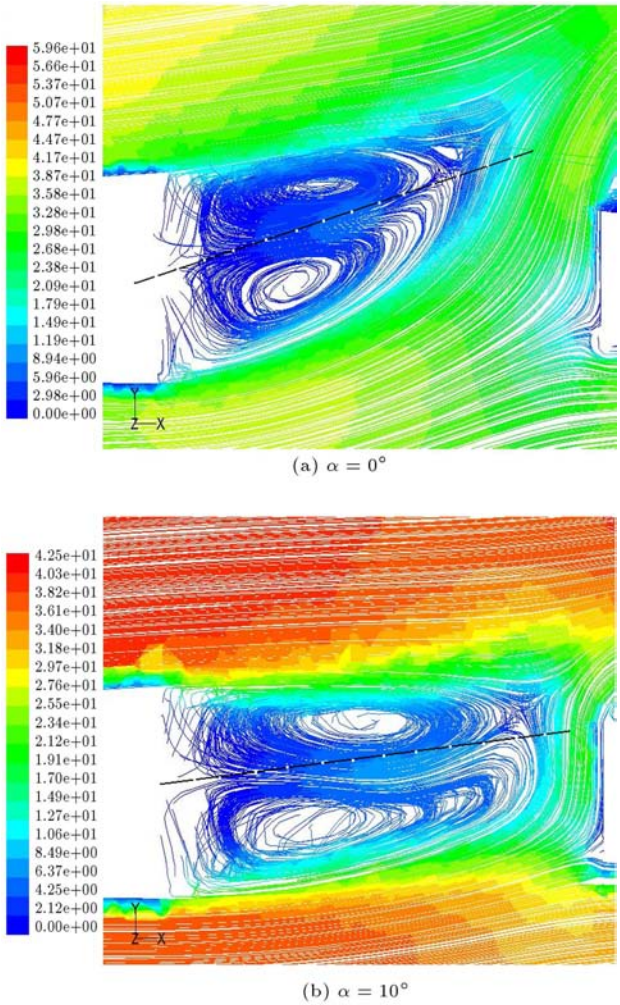

Figure 11. Path lines inside the cavity of circle damage.

the slope of these curves. Compared to the circle and right triangle, the delayed onset of the strong jet for the inversed triangle results in the smaller drag increments and reduced lift and pitching moment increments.

The effect of a wall on aerodynamic coefficients is shown in Figure 15. Close to the stall, there is some uncertainty about the accuracy of the results, since existence of a large amount of separated flow makes the application of wind tunnel correction difficult [10,11]. It is seen that the effect of the upper and lower walls of the test section on the lift coefficients of the damaged airfoil is to increase it at higher angles of attack. This result is also expected from undamaged airfoil, due to increasing the velocity of the free stream near the surface of the airfoil, the solid blockage and wake blockage effects [12]. For comparison, aerodynamic coefficient increments versus angle of attack are shown in Figure 14. As seen, the existence of the wall resulted in more negative aerodynamic coefficient increments. This means that the influence of walls is more pronounced in a damaged airfoil than an undamaged one.

In Figure 16, a comparison between numerical and experimental results [7] is shown for the case of 'without wall'. It is the lift coefficient increment versus α, which relates to the loss of lift due to the right triangle damage. The percentage of deviation between two sets of results is about 2% on average. It is seen that there is a good agreement between numerical and experimental results, quantitatively.

CONCLUSION

Circle, right and inverse triangle damaged airfoils were numerically modeled and the resulting flow fields were investigated. As the flow passes through the damage hole, depending on the incidence angle, a weak or strong jet may be formed. Weak-jets formed an attached wake and resulted in small changes in force and moment coefficients. Strong-jets resulted from increased incidence where through flow penetrated into the free stream flow resulting in separation of the oncoming surface flow and the development of a larger separated wake with reverse flow. The effect on force

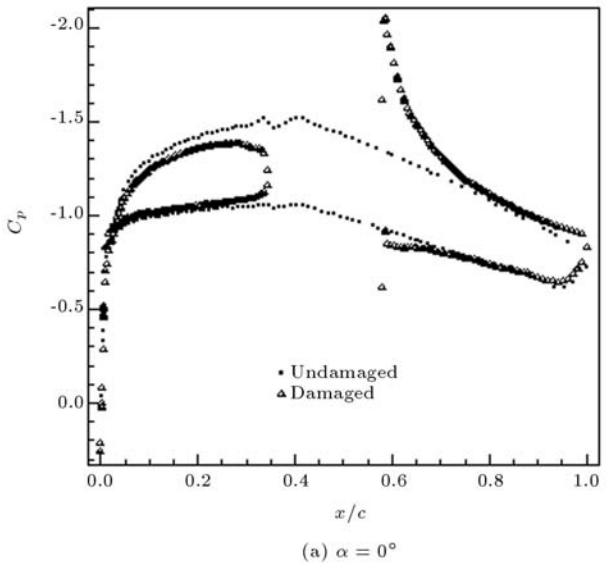

(a) $\alpha = 0°$

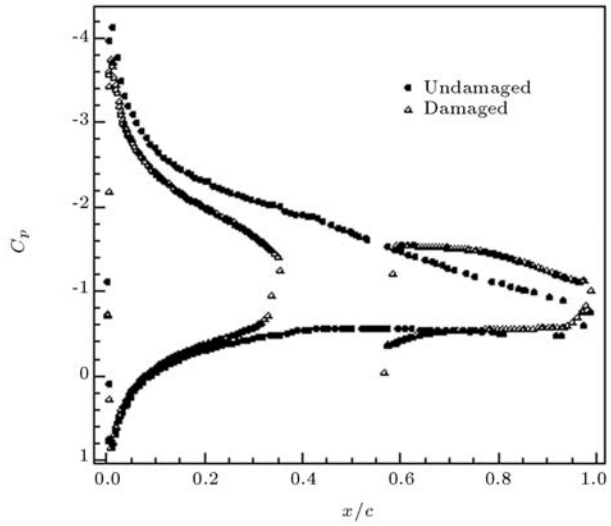

(b) $\alpha = 10°$

Figure 12. Effect of damage on pressure distribution.

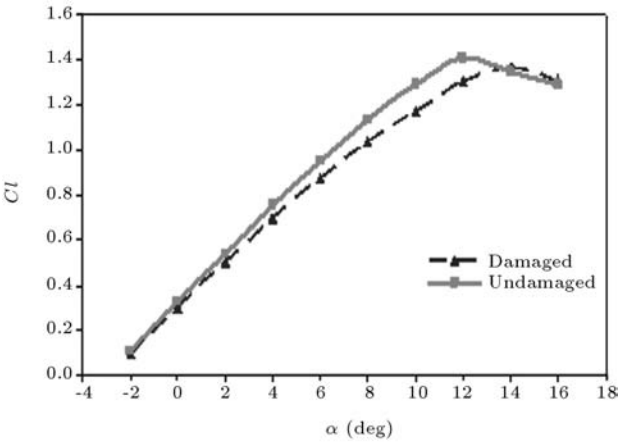

Figure 13. Lift coefficients of damaged (right triangle) and undamaged airfoil.

and moment coefficients was significant. Thus, as the angle of attack was increased, pressure differential increased, and hence jet velocity increased (relative to the wing free stream velocity). For a fixed angle of attack, the jet size was dependent on the shape of the damage. In fact, its size was determined by the

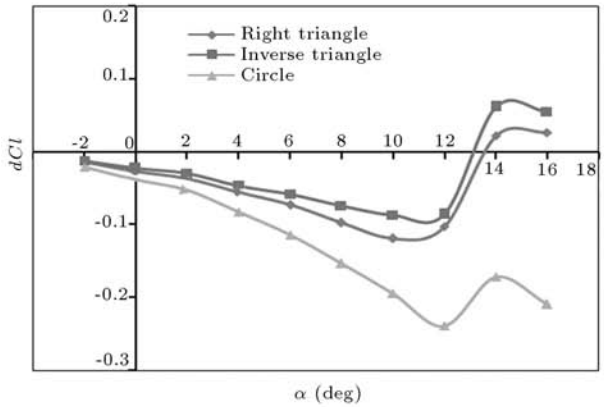

(a) Lift coefficient

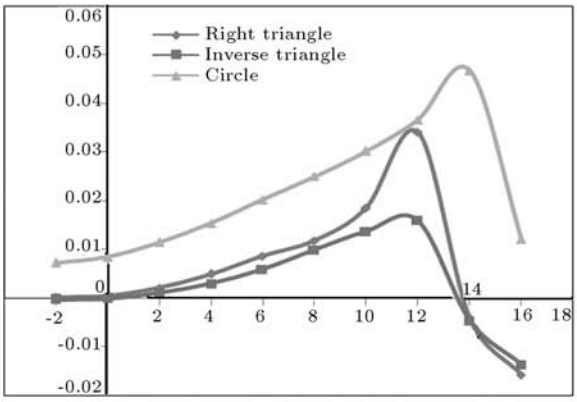

(b) Drag coefficient

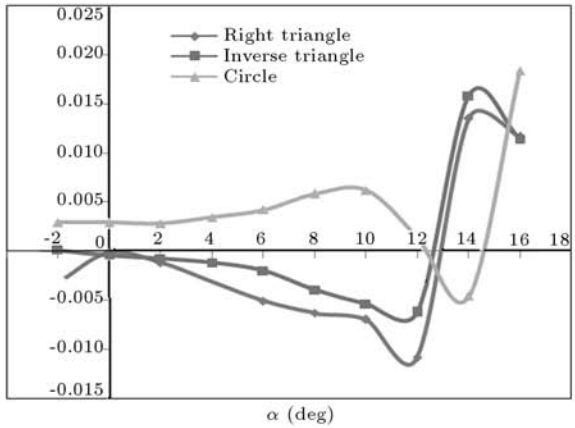

(c) Pitching moment coefficient

Figure 14. Aerodynamic coefficient increments due to three different damage shapes.

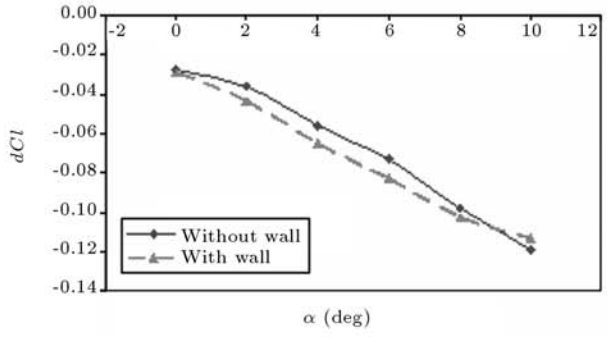

(a) Lift coefficient increment

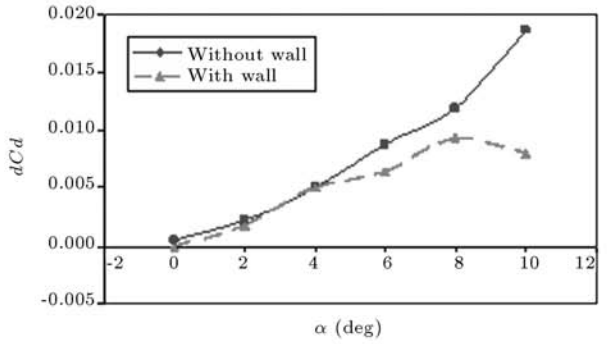

(b) Drag coefficient increment

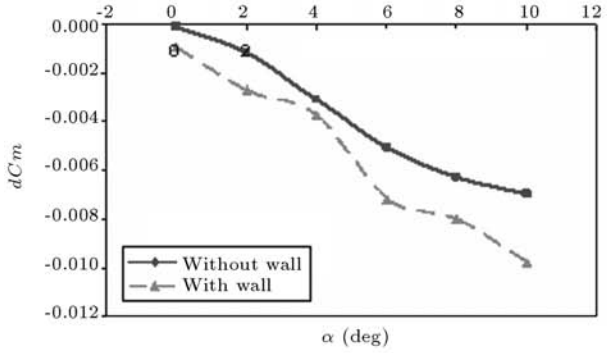

(c) Pitching moment coefficient increment

Figure 15. Wall effect on aerodynamic coefficient increments (right triangle damage).

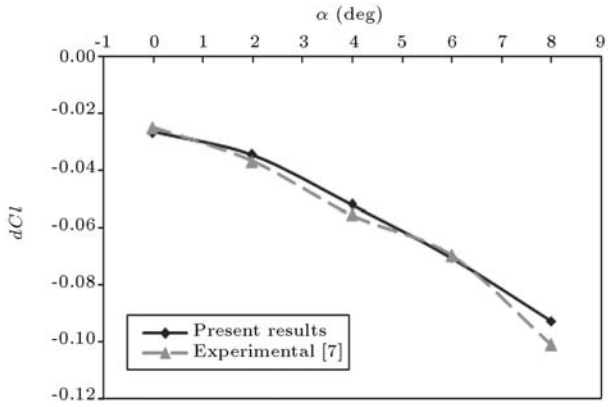

Figure 16. Comparison of results with experimental data.

width of the rear part of the hole. Compared to the circle and right triangle, the delayed onset of the strong jet for the inversed triangle resulted in the smaller drag increments and reduced lift and pitching moment increments. The effects of a wall included increasing the lift and moment coefficients at higher angles of attack and more pronounced effects on damaged airfoil aerodynamic coefficients.

REFERENCES

1. Irwin, A.J. "Investigation into aerodynamic effects of simulated battle damage to a wing", PhD Dissertation, Loughborough University, Loughborough, UK (1998).
2. Hayes, C. "Effects of simulated wing damage on the aerodynamic characteristics of a swept-wing airplane model", NASA TMX-1550 (1968).
3. Irwin, A.J., Render, P.M., McGuirk, J.J., Probert, B. and Alonze, P.M. "Initial investigation into aerodynamic properties of a battle damaged wing", *13th AIAA Applied Aerodynamics Conference*, AIAA95-1845, San Diego, California, USA (June 1995).
4. Irwin, A.J. and Render, P.M. "The influence of internal structure on the aerodynamic characteristics of battle-damaged wings", *14th AIAA Applied Aerodynamics Conference*, AIAA96-2395, New Orleans, USA (June 1996).
5. Robinson, K.W. and Leishman, J.G. "The effects of ballistic damage on the aerodynamics of helicopter rotor airfoils", *Proceeding of the American Helicopter Society, 53rd Annual Forum* (1997).
6. Render, P.M. and Walton, A.J. "Aerodynamics of battle damaged wings- The influence of flaps, camber, and repair schemes", *23rd AIAA Applied Aerodynamics Conference* (2005).
7. Mani, M. and Render, P.M. "Experimental investigation into the aerodynamic characteristics of airfoils with triangular and star shaped through damage", *23rd AIAA Applied Aerodynamics Conference*, AIAA-2005-4978, Toronto, Ontario (2005).
8. Andreopoulos, J. and Rodi, W. "Experimental investigation of jets in a crossflow", *J. Fluid Mech.*, **138**, pp. 93-127 (1984).
9. Ajersch, P., Zhou, J.M., Ketler, S., Salcudean, M. and Gartshore, I.S. "Multiple jets in a crossflow: Detailed measurements and numerical simulations", *ASME- 95-GT-9*, pp. 1-16 (1995).
10. Rasi Marzabadi, F., Ajalli, F., Mani, M. and Taeibi Rahni, M. "Numerical aerodynamic analysis of a damaged airfoil", *25th AIAA Applied Aerodynamics Conference*, AIAA-2007-4180, Hyatt Regency Miami, Miami, FL (June 2007).
11. Rasi Marzabadi, F., Ajalli, F., Mani, M. and Taeibi Rahni, M. "Numerical aerodynamic analysis of a damaged airfoil with wall effects", *5th International Conference on Heat Transfer, Fluid Mechanics and Thermodynamics*, HEFAT2007-SM5, Sun City, South Africa (2007).

12. ESDU "Lift-interference and blockage corrections for two-dimensional subsonic flow in ventilated and closed wind-tunnels", Item No. 76028, Engineering Science Data Unit (2004).

BIOGRAPHIES

Faezeh Rasi Marzabadi received her B.S. degree in Aerospace Engineering from Amirkabir University of Technology in 2003, and a M.S. degree in Aerodynamics, in 2005, from Sharif University of Technology, where she is now a Ph.D. student of Aerodynamics. Her research interests are in Applied Aerodynamics, Experimental and Numerical Fluid Dynamics and Wind Tunnel Testing. She has published several papers in various international conferences and journals.

Behnaz Beheshti Boroumand received her B.S. and M.S. degrees in Aerospace Engineering in 2001 and 2003, respectively, from Amirkabir University of Technology, Tehran, Iran, where she is now a Ph.D. student. Her research interests are in Experimental and Numerical Fluid Dynamics and Applied Aerodynamics. She has published several papers in various international conferences and journals.

Mahmoud Mani is a Professor of Aerospace Engineering in Amirkabir University of Technology, Tehran, Iran, obtaining his M.S. degree in Aerospace Engineering and Ph.D. in Applied Mechanics (Aerodynamics) from E.N.S.A.E, Toulouse, France. His research areas are in Aerodynamic Design and Wind Tunnel Testing. He has published more than 75 papers in various conferences and journals in areas of Mechanical and Aerospace Engineering.

Fariba Ajalli received her B.S. degree in Mechanics from Mazandaran University in 2003 and her M.S. degree in Aerodynamics from Amirkabir University of Technology in 2006, where she is now a Ph.D. student. Her research interests are in Experimental and Numerical Fluid Dynamics, and Applied Aerodynamics. She has published several papers in various international conferences and journals.